Solar radiation research for photovoltaic applications

C. Riordan, R. Hulstrom, T. Cannon and **D. Myers**
Solar Energy Research Institute, 1617 Cole Boulevard, Golden, CO 80401 (U.S.A.)

(Received October 25, 1990)

Abstract

This paper gives an overview of the fiscal year 1990 research activities and results under the Solar Radiation Research Task of the Photovoltaic Advanced Research and Development Project at the Solar Energy Research Institute. The activities under this task include developing and applying measurement techniques, instrumentation, and data analysis and modeling to understand and quantify the response of photovoltaic devices to variations in broad-band and spectral solar radiation.

1. Introduction

The purpose of the Solar Radiation Research Task under the Photovoltaic (PV) Advanced Research and Development Project at the Solar Energy Research Institute is to support the national PV program by helping to develop a fundamental scientific understanding of the relationships between the natural broad-band and spectral solar radiation environment and the design, performance, and performance measurements of PV devices. The task addresses the needs expressed by the PV community for instrumentation, data and models, and measurement and analysis techniques to understand the response of PV devices to variations in broad-band and spectral solar radiation [1–3].

This paper gives an overview of the key activities and results in fiscal year 1990 under the Solar Radiation Research Task. The activities include further developing the Atmospheric Optical Calibration System (AOCS), spectroradiometry, plane-of-array solar irradiance measurements, PV device spectral sensitivity and measurement techniques, and measurement support and technology transfer.

2. Atmospheric optical calibration system

The AOCS (Fig. 1) is an instrument designed to provide real-time information on atmospheric optical conditions, such as haziness (turbidity) and water vapor, and solar radiation conditions that affect PV device performance during outdoor tests [4, 5]. A patent, No. 4 779 980, was issued on the system on October 25, 1988. A prototype AOCS working unit (including basic software) was designed and constructed in 1988, followed by extensive

0379-6779/91/$3.50

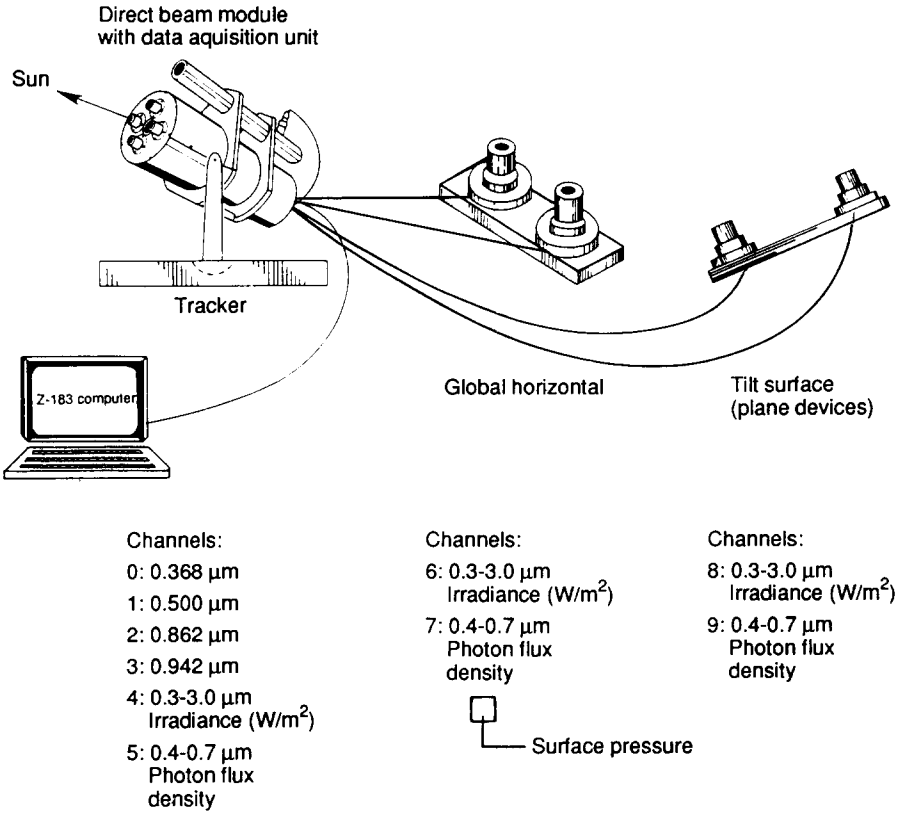

Fig. 1. Schematic and schematic of the AOCS components and schematic of the AOCS direct-beam module.

laboratory testing in 1989. In 1990, the AOCS working unit was calibrated and tested outdoors and additional software was developed. Outdoor calibrations were performed for the narrow-wavelength (10 nm) channels at 368, 500 and 862 nm; data from these channels are used to calculate atmospheric aerosol effects (turbidity). Very repeatable (0.5–3% standard deviation, depending on the channel) calibration factors were obtained, which is important for maximizing the sensitivity of these channels to the atmospheric aerosol effects. Software was written so that the calibration data can be acquired with the AOCS in an unattended mode; this allows the operator to check the calibration frequently when the AOCS is operated routinely. Additional software is being added to temperature-correct the AOCS data based on laboratory test data.

A major research activity in the final AOCS software development is the modification of an algorithm to calculate precipitable water vapor from AOCS data at 862 nm (outside the absorption bands for atmospheric water vapor) and 940 nm (inside a water vapor absorption band). A measure of water vapor is important because most atmospheric water vapor absorption occurs

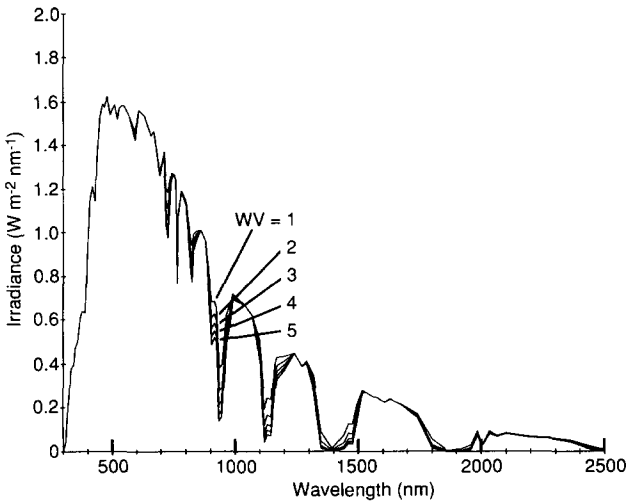

Fig. 2. Water vapor absorption for different amounts (precipitable centimetres) of water vapor, simulated using a spectral irradiance model.

in the near-infrared (NIR) region of the spectrum (Fig. 2); therefore, it affects the relative spectral irradiance distribution between the visible and NIR regions. The effects of water vapor variations on a PV device depend on the device's spectral response. If the spectral response of a PV device extends into the NIR region, the device's short-circuit current will be affected by water vapor variations. If the spectral response of a PV device does not extend into the NIR region, the calculated device efficiency will be affected by water vapor variations because the total irradiance (the denominator in efficiency calculations) will vary.

In 1990, we obtained balloon sonde data from the National Oceanic and Atmospheric Administration. We are using the data to examine how sensitive atmospheric water vapor transmittance is to the vertical profile of water vapor, temperature, and pressure, as well as to surface temperature and pressure. The algorithm in the AOCS software for calculating the transmittance of atmospheric water vapor requires fixed pressure and temperature values, so the results of this study are important for understanding the sensitivity and accuracy of the AOCS water vapor calculation.

3. Spectroradiometry

PV cell efficiency measurements are usually referenced to a particular spectrum so that results can be compared among various laboratories. Spectral irradiance is measured during the cell performance tests and is used to translate the test results to the reference spectrum. Spectroradiometers with a wavelength range of 290–4000 nm are desirable to cover the wavelength response of all PV devices and to integrate the entire solar spectrum to

obtain total irradiance. Otherwise, models must be used to extend the measured spectrum to cover the entire spectral region.

A technical challenge in spectroradiometry for PV applications is to develop an extended-wavelength spectroradiometer with a fast time response (1 ms for measuring flash simulators to less than 1 min to measure outdoor spectra) with repeatability and accuracy within at least 5% (ideally 1%) over the entire spectral range. In addition, different front-end optics are needed for outdoor solar spectral irradiance measurements of the sun's disk (direct-beam irradiance in a 5° field of view) or the sky hemisphere (global irradiance from the sky hemisphere, with the direct beam at various incidence angles), without compromising the spectral measurement accuracy.

Spectroradiometers with user-friendly operating software are commercially available to measure the range 400–1100 nm with a wavelength-dependent accuracy of approximately 3–10%. At SERI, we are currently using these spectroradiometers with a view-limiting tube (which restricts the field of view to match that of the absolute cavity radiometer) to measure direct-beam solar spectral irradiance during outdoor PV tests; we also use a model to extend the measurements beyond 1100 nm [6].

Solar spectral irradiance measurements outside the 400–1100 nm wavelength range are more difficult and require more complex spectroradiometers. We are pursuing two options at SERI. One is to modify a spectroradiometer originally designed for geophysical applications. We are currently using this instrument to measure simulator spectral irradiance between 300 and 3000 nm in a single scan that takes about 3.5 min. The measurement accuracy of this instrument is acceptable (better than 5%), except in the ultraviolet region. An integrating sphere was designed for the unit, but signal levels using the sphere have not been acceptable and therefore more work is needed. Work on this instrument has been temporarily delayed to pursue a second option, which is to develop an EG&G optical multichannel analyzer (OMA III) for solar spectral measurements.

The OMA uses a 1024-element silicon (285–1100 nm spectral range) detector array, which allows all wavelengths to be measured simultaneously in less than 1 ms. A separate 256-element Ga/In/As detector array allows the 800–1750 nm spectral range of the pulsed simulators to be measured. This has the advantage over the conventional spectroradiometer of allowing accurate measurements of pulse sources as well as spectrally unstable outdoor conditions. A measurement of SERI's SPIRE 240A pulse simulator is shown together with the American Society for Testing and Materials (ASTM) air mass 1.5 global standard spectrum (E892-87) in Fig. 3(a). Integrating the simulator spectrum over the ASTM E927 solar simulation standard bandwidths (Figure 3(b)) shows that the SPIRE simulator meets Class A spectral-content requirements, except in the 800–900 nm range, which is probably within the uncertainty limits of the measurement.

Calculating the spectral measurement uncertainty of spectroradiometers is a complex, non-standard procedure [7, 8]. To assess the state of the art in spectral measurement uncertainty, we participated in (and helped sponsor)

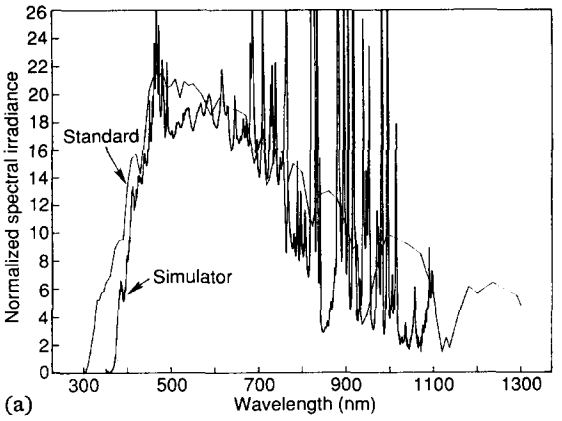

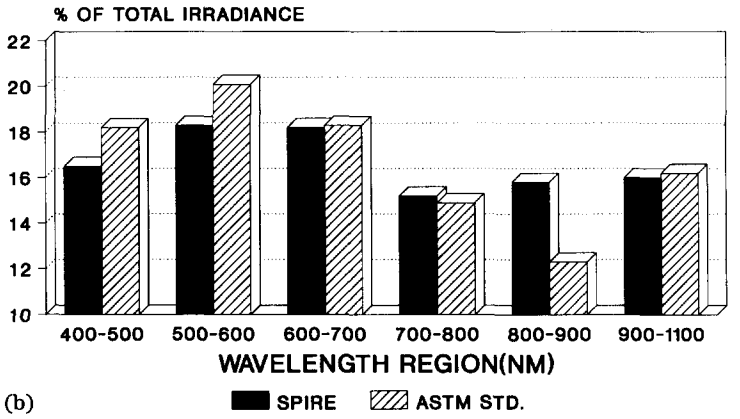

Fig. 3. Comparison of SERI's SPIRE 240A pulse simulator with the American Society for Testing and Materials air mass 1.5 global standard spectrum.

a spectroradiometer intercomparison at DSET Laboratories in Phoenix, AZ, in April 1990. The participants included experts from four environmental testing laboratories in the United States, as well as from SERI and the National Institute of Standards and Technology. In brief, the objectives of the intercomparison were to compare measurement results from SERI spectroradiometers with results from other laboratories; gather experts together from a few laboratories to improve spectroradiometry information transfer; provide an opportunity to acquire some of the measurements required to begin development of national and international spectroradiometry standards; and improve and document procedures for conducting spectroradiometer intercomparisons.

During the intercomparison, outdoor solar spectral measurements were taken in global and direct-normal modes, and indoor measurements were taken of two ultraviolet-enhanced fluorescent sources and three phosphor colors. All results of this intercomparison are confidential at this time; certain results will be released at a later date.

4. Plane-of-array solar irradiance measurements

A key variable in systems analysis of various PV collector options (concentrators, two-axis and one-axis tracking flat plates, and fixed-tilt flat plates) is the plane-of-array (POA) irradiance. Systems analysis, with irradiance as one of the input variables, is used to compare the cost of more expensive and complex collector options (like two-axis tracking compared with fixed tilt) with the value of increased PV power output resulting from the irradiance enhancement.

In 1990, we examined data from various published studies and outdoor measurement programs on POA irradiance or PV energy output (which is dominated by POA irradiance), to show the relationship between potential irradiance enhancements for various collector options and site cloudiness. Ratios of POA irradiance for pairs of collector options indicate potential enhancements (*e.g.* 7.5 kW h m^{-2} per day/7.0 kW h m^{-2} per day is 1.07, or an enhancement of 7%). As a measure of site cloudiness, we used a variable called the cloudiness index (K_t), which is global-horizontal irradiance divided by extraterrestrial irradiance on a horizontal surface. This variable is a measure of bulk atmospheric transmittance, which varies with different atmospheric conditions. K_t varies with sun angle (or air mass), but its average annual value is dominated by the site's cloudiness. A map of the average annual K_t for the United States [9] is shown in Fig. 4.

Annual average daily global POA irradiance values calculated by Sandia National Laboratories [10] for different types of collector options are divided by direct-normal values from the Sandia report, and the ratios are shown in Fig. 5(a) as a function of average annual K_t. A simple regression of the irradiance ratios and K_t shows the strong inverse relationship. As expected, the ratio of global POA irradiance to direct-normal POA irradiance is a strong function of cloudiness because there is no direct-beam irradiance when the sky is overcast. The ratios of pairs of global POA irradiance values (Figs. 5(b) and 5(c) show less K_t dependence than the ratios for global compared with direct normal. The quadratic fits to the global ratios as a function of K_t do not have high correlation coefficients because there is much scatter in the ratios, but they do show relative trends in the data and the magnitude of potential irradiance enhancements.

For broad-scale assessments of potential POA irradiance enhancements in various climate regions of the United States, one can use the K_t map (Fig. 4) with average enhancement factors *vs.* K_t (Fig. 5). This method is by no means appropriate for site-specific analysis. In all cases of site-specific economic systems analysis, one should obtain local (regional) irradiance data and calculate (or use measured) POA irradiance for each collector option, including flat plates with optimized tilt angles (instead of tilt equals latitude) and concentrators with specific apertures and concentration ratios. The POA irradiance data should be combined with other data, such as reflection losses at non-zero incidence angles [11], to obtain the most reliable comparison of collector options. Seasonal variations in the enhancements should be

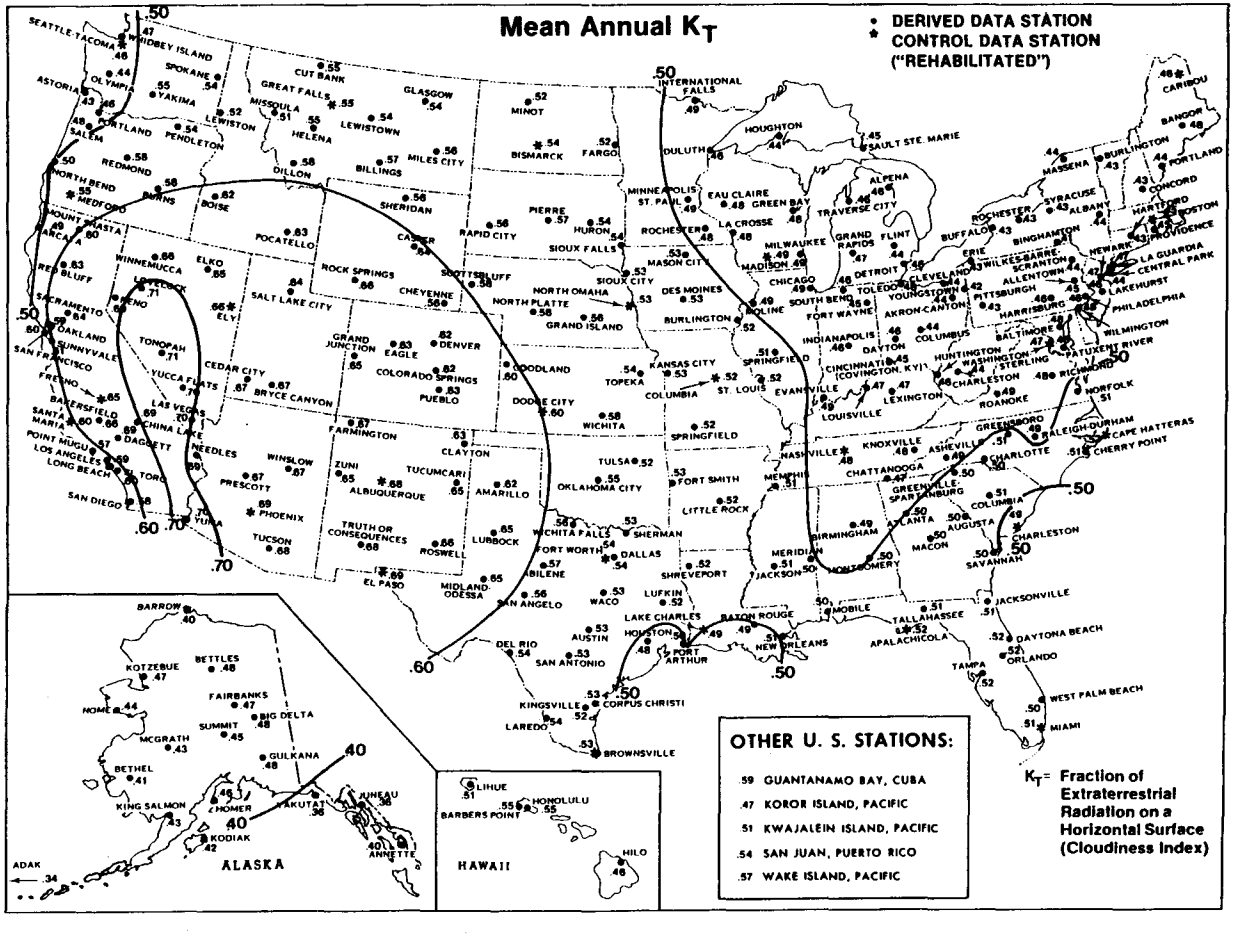

Fig. 4. Cloudiness index (K_t) map for the United States [9].

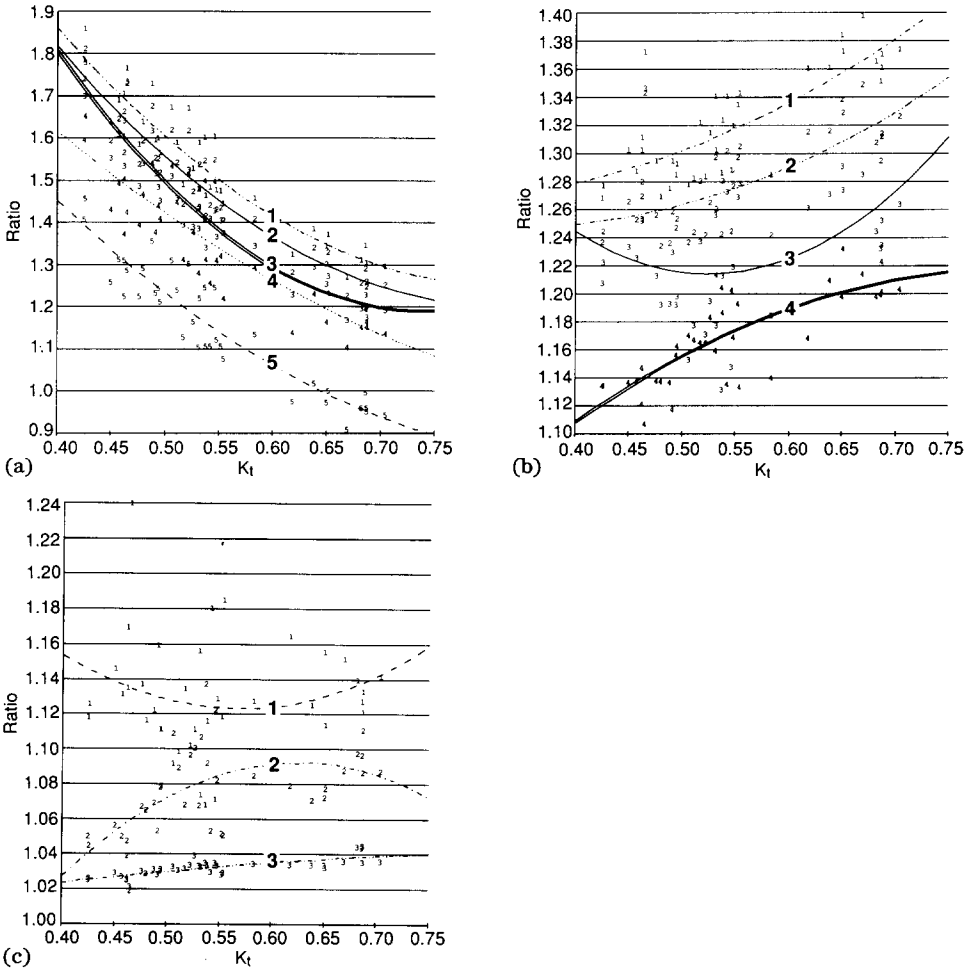

Fig. 5. Ratios for global POA irradiance for (a) five flat-plate collector options, divided by direct-normal POA irradiance; (b) four flat-plate tracking options, divided by global POA irradiance for a flat plate with a fixed tilt at the latitude; (c) two-axis tracking flat plate, divided by global POA irradiance for three one-axis options. The numerators in (a) and (b), and denominators in the ratios in (c) are: 1, two-axis tracking; 2, one-axis tracking, axis oriented north–south, and collectors tilted at the latitude; 3, one-axis tracking, vertical axis, and collectors tilted at the latitude; 4, one-axis tracking, axis oriented north–south, and collectors horizontal; 5, fixed tilt at latitude.

analyzed, especially for evaluating the electric load matching potential of PV.

5. PV device spectral sensitivity and measurement techniques

Methods are needed to quantify the sensitivity of PV device performance to natural spectral solar irradiance variations because PV devices are spectrally

selective [12]. Although PV device measurements are often corrected to a reference spectrum to compare results among laboratories, the reverse calculations are usually not performed to predict performance for a range of spectral irradiance conditions or to put "error bars" on performance measurements. Measurements or modeling should be performed in the design phase to determine whether or not the PV device performance will be adversely affected by spectral irradiance variations, especially for series-connected multijunction devices that require current matching for optimum performance.

One way to examine spectral sensitivity is to calculate PV device performance using a device model together with a spectral irradiance model or data base for different atmospheric conditions and air masses; a second way is to perform outdoor tests under different spectral irradiance conditions. For the first approach, SERI's spectral irradiance model and data base [13, 14] are made available to any user who wants to perform these analyses. The second approach is time consuming if outdoor measurements are made for a full range of atmospheric conditions and air masses.

Although spectroradiometers are available for measuring spectral irradiance during outdoor tests, they are not used routinely to report spectral effects in outdoor PV device performance tests. Simple and economical methods and instruments are needed to measure first-order (coarse) solar spectral irradiance variations (at least until instruments like the AOCS are commercially available).

A simple method for monitoring first-order spectral irradiance variations is to measure irradiance using filtered and unfiltered radiometers, which separate the spectrum into roughly visible (<780 nm) and NIR (>780 nm) regions [15]. Such measurements have been taken at SERI since the summer of 1988.

Figures 6 and 7 give examples of the information on spectral irradiance variations that can be derived from filtered and unfiltered pyrheliometer and pyranometer data. Figure 6, for a clear day, shows the total irradiance and the ratio of NIR to total irradiance for direct-normal (left) and global-horizontal (right) cases. In the early morning and late afternoon, the NIR fraction of

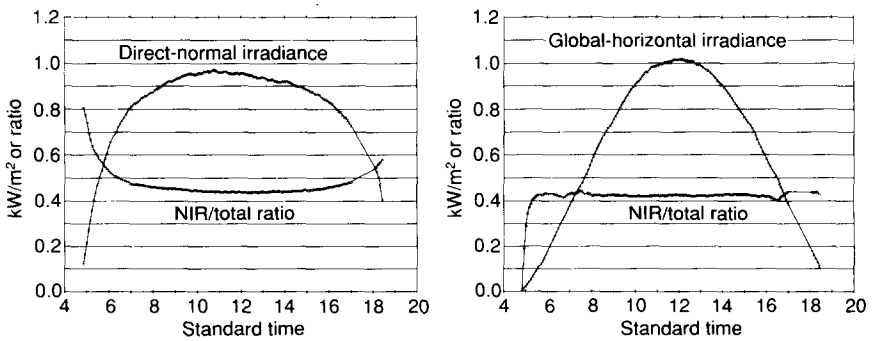

Fig. 6. Total irradiance and the ratio of NIR to total irradiance on a clear day in Golden, CO, for direct-normal (left) and global-horizontal (right) cases.

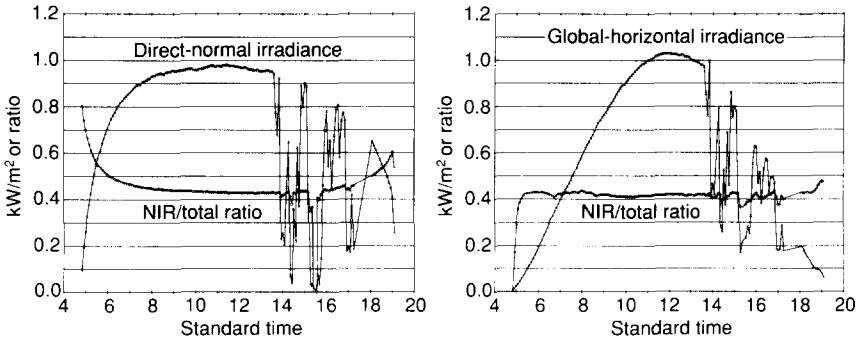

Fig. 7. Total irradiance and the ratio of NIR to total irradiance on a partly cloudy day in Golden, CO, for direct-normal (left) and global-horizontal (right) cases.

total irradiance increases for the direct-normal case (from high air mass or low sun elevation effects) while the midday ratio remains relatively constant. The midday ratio may vary from day to day depending on atmospheric water vapor and aerosol effects. For the global-horizontal case, the midday ratio is relatively constant with a slight increase at the ends of the day.

Figure 7, for a partly cloudy day, shows patterns similar to those of the clear day except that the direct-normal ratio is too unstable to be reliable when clouds obscure the sun's disk (because the irradiance values in the ratios are very small), and the global-horizontal ratios decrease slightly when clouds reduce the irradiance (probably because of increased water vapor and liquid water absorption in the clouds [16]).

The extent to which a PV device is affected by changes in the distribution of irradiance between the NIR and visible regions (visible fraction equals one minus the NIR fraction) depends on the spectral response (or quantum efficiency) of the PV device, or where it overlaps the visible and NIR regions of the spectrum. If PV device performance and the fraction of visible *vs.* NIR irradiance are monitored simultaneously during outdoor tests, a sensitivity study can be performed to quantify the relationships.

6. Measurement support and technology transfer

Other activities under the Solar Radiation Research Task include operating the Solar Radiation Research Laboratory, an outdoor laboratory used for radiometer and PV cell calibrations and for performing special experiments; presenting papers at conferences [8, 17, 18]; and providing expertise, data and models on spectral solar irradiance as related to PV applications.

7. Summary

Resources allocated to the Solar Radiation Research Task of the Photovoltaic Advanced Research and Development Project support about two

research staff persons at the Solar Energy Research Institute. The research performed under this task is directed toward understanding and quantifying the relationship between PV device performance and spectral and broadband solar irradiance variations. To develop this scientific understanding, the research staff members develop instruments (such as the AOCS and spectroradiometers) and solar irradiance measurement and analysis methods (such as simple methods for monitoring first-order spectral irradiance variations and investigations of the climate dependence of POA irradiance enhancements for various collector options), and they provide analytical and measurement support regarding solar irradiance for PV device design and performance tests.

References

1 R. L. Hulstrom, T. W. Cannon and C. J. Riordan, Photovoltaic Advanced Research and Development Project, Solar Radiation Research, Annual Report for 1 October 1986–30 September 1987, SERI/PR-215-3297, SERI, Golden, CO, March 1988.

2 C. J. Riordan, R. L. Hulstrom, T. W. Cannon, T. L. Stoffel and D. R. Myers, Photovoltaic Advanced Research and Development Project Solar Radiation Research Task, Annual Report for 1 October 1987–30 September 1988, SERI/TR-215-3445, SERI, Golden, CO, February 1989.

3 C. Riordan, R. Hulstrom, T. Cannon, D. Myers and T. Stoffel, Photovoltaic Advanced Research and Development Project: Solar Radiation Research Annual Report, 1 October 1988–30 September 1989, SERI/PR-215-3607, SERI, Golden, CO, February 1990.

4 T. W. Cannon and R. L. Hulstrom, A multi-channel radiometer for measurement of the optical properties of the atmosphere, in *Optical Radiation Measurements II*, Proc. SPIE, Vol. 1109, The Society of Photo-Optical Instrumentation Engineers, Bellingham, WA, 1989, pp. 152–159.

5 T. W. Cannon and R. L. Hulstrom, Specialized instrumentation and techniques for measurement of terrestrial solar radiation, in *Proc. Daylight and Solar Radiation Measurement Conf., October 9–11, 1989, Berlin, Germany*, Institut für Lichttechnik, Technische Universität Berlin, Einsteinufer 19, D-1000 Berlin 10, pp. 312–321.

6 C. Osterwald, K. A. Emery, D. R. Myers and C. J. Riordan, Extending the spectral range of silicon-based direct-beam solar spectral radiometric measurements, in *20th IEEE PV Specialists Conf.*, IEEE, New York, 1988, pp. 1246–1250.

7 D. R Myers, Estimates of uncertainty for measured spectra in the SERI spectral solar radiation data base, *Sol. Energy, 43* (1989) 347–357.

8 D. Myers, Principles of uncertainty analysis with examples drawn from radiometry, presented at the CORM 90 Annual Meeting, May 9–11, 1990, Rochester, New York, unpublished material, SERI, Golden, CO.

9 Solar Technical Information Program, Insolation Data Manual and Direct Normal Solar Radiation Data Manual, SERI/TP-220-3880, SERI, Golden, CO, July 1990.

10 D. F. Menicucci and J. P. Fernandez, Estimates of Available Solar Radiation and Photovoltaic Energy Production for Various Tilted and Tracking Surfaces Throughout the U.S. Based on PVFORM, A Computerized Performance Model, SAND85-2775, SNL, Albuquerque, NM, March 1986.

11 S. Nann, Potentials for tracking photovoltaic system and V-troughs in moderate climates, *Solar Energy*, submitted for publication.

12 C. J. Riordan and R. L. Hulstrom, Summary of Studies that Examine the Effects of Spectral Solar Radiation Variations on PV Device Design and Performance, SERI/TR-215-3437, SERI, Golden, CO, March 1989.

13 R. E Bird and C. Riordan, Simple solar spectral model for direct and diffuse irradiance on horizontal and tilted planes at the earth's surface for cloudless atmospheres, *J. Climate Appl. Meteorol.*, *25* (1986) 87–97.
14 C. Riordan, D. Myers and R. Hulstrom, Spectral Solar Radiation Data Base Documentation and User's Manual, Vols. I and II, SERI/TR-215-3513, SERI, Golden, CO, January 1990.
15 C. Riordan and D. Myers, Using Filtered and Unfiltered Radiometers to Monitor Spectral Solar Radiation Conditions During Outdoor Photovoltaic Tests, SERI/TP-215-4001, SERI, Golden, CO, draft.
16 S. Nann and C. Riordan, Solar spectral irradiance under overcast skies, in *21st IEEE PV Specialists Conf., Orlando, FL, May 1990*, IEEE, New York, pp. 1110–1115.
17 C. Riordan and R. Hulstrom, What is an air mass 1.5 spectrum?, in *21st IEEE PV Specialists Conf., Orlando, FL, May 1990*, IEEE, New York, pp. 1085–1088.
18 C. R. Osterwald, K. A. Emery, D. R. Myers and R. E. Hart, Primary reference cell calibrations at SERI: history and methods, in *21st IEEE PV Specialists Conf., Orlando, FL, May 1990*, IEEE, New York, pp. 1062–1067.